MPMI Vol. 30, No. 12, 2017, pp. 984–996. https://doi.org/10.1094/MPMI-03-17-0067-R

e-Xtra*

Histochemical Analyses Reveal That Stronger Intrinsic Defenses in *Gossypium barbadense* Than in *G. hirsutum* Are Associated With Resistance to *Verticillium dahliae*

Yan Zhang, Xingfen Wang, Wei Rong, Jun Yang, Zhikun Li, Liqiang Wu, Guiyin Zhang, and Zhiying Ma†

Department of Agronomy, North China Key Laboratory for Germplasm Resources of Education Ministry, Hebei Agricultural University, Baoding 071001, People's Republic of China

Accepted 25 August 2017.

Verticillium wilt, caused by *Verticillium dahliae* Kleb., is a serious threat to cotton (*Gossypium* spp.) crop production. To enhance our understanding of the plant's complex defensive mechanism, we examined colonization patterns and interactions between *V. dahliae* and two cotton species, the resistant *G. barbadense* and the susceptible *G. hirsutum*. Microscopic examinations and grafting experiments showed that the progression of infection was restricted within *G. barbadense*. At all pre- and postinoculation sampling times, levels of salicylic acid (SA) were also higher in that species than in *G. hirsutum*. Comparative RNA-Seq analyses indicated that infection induced dramatic changes in the expression of thousands of genes in *G. hirsutum*, whereas those changes were fewer and weaker in *G. barbadense*. Investigations of the morphological and biochemical nature of cell-wall barriers demonstrated that depositions of lignin, phenolic compounds, and callose were significantly higher in *G. barbadense*. To determine the contribution of a known resistance gene to these processes, we silenced *GbEDS1* and found that the transformed plants had decreased SA production, which led to the upregulation of *PLASMODESMATA-LOCATED PROTEIN* (*PDLP*) *1* and *PDLP6*. This was followed by a decline in callose deposition in the plasmodesmata, which then led to increased pathogen susceptibility. This comparison between resistant and susceptible species indicated that both physical and chemical mechanisms play important roles in the defenses of cotton against *V. dahliae*.

Cotton (*Gossypium* spp.) is one of the most important cash crops, supplying approximately 35% of the total fiber used worldwide (United States Department of Agriculture Economic Research Service 2013). Cotton (*Gossypium* spp.) is one of the most important cash crops, supplying spinning fiber that has economic significance worldwide. The second major species, *G. barbadense* (Sea Island cotton), accounts for nearly 3% of the world's cotton production (Zhang et al. 2014). Although both species have a common ancestor (Wendel and Cronn 2003), they have diverged with respect to many agronomic traits. For example, *G. hirsutum* is high-yielding in a wider range of climates but is generally susceptible to Verticillium wilt, while *G. barbadense* has superior fiber quality and shows strong resistance to Verticillium wilt and root-knot nematode (Wilhelm et al. 1972, 1974).

Verticillium wilt is one of the most important diseases in cotton and is especially destructive in *G. hirsutum* (Cai et al. 2009). Plants are susceptible at any developmental stage and can display symptoms such as leaf curl, defoliation, and discoloration of vascular tissues (Cai et al. 2009; Sink and Grey 1999). Most regions where cotton is grown are threatened and significant losses to both yield and quality have been reported. For example, more than 2 million hectares have been affected in China, and severe disease outbreaks have reduced yields by up to 30% (Cai et al. 2009). This wilt is caused by *Verticillium dahliae* Kleb., a soil-borne vascular wilt fungus that survives in the soil as hardened microsclerotia. Upon sensing a root nearby, the microsclerotia germinate to hyphae that invade plants through the root tips or at the site of lateral root formation (Fradin and Thomma 2006). *V. dahliae* establishes infection when it crosses the plant endodermis and enters the vascular tissues. After 2 to 4 days, the fungus enters the xylem elements and sporulates. The conidia are disseminated through the xylem and the shoots. Colonization of the xylem tissue can interrupt the transpiration stream and produces the wilt symptoms commonly associated with the disease. As the disease progresses, the pathogen produces large amounts of microsclerotia in necrotic or senescing tissue (Chen et al. 2004; Fradin and Thomma 2006; Gold and Robb 1995; Heinz et al. 1998).

Plants generally use both physical (constitutive) and biochemical (induced) defenses against microbes (Glazebrook 2005). The cell wall, especially the pectin, cellulose, and lignin components, presents the most important pre-existing physical barrier (Eggert et al. 2014; Ellinger et al. 2013). As one of many induced responses, strengthening of those barriers is regulated by a sophisticated signaling network centered on phytohormones salicylic acid (SA), jasmonic acid (JA), and ethylene (ET) (Durrant and Dong 2004; Fu et al. 2012; Hamann 2012; Jones and Dangl 2006; Malinovsky et al. 2014; Moore et al. 2011).

SA is involved in the activation of responses against biotrophic and hemibiotrophic pathogens as well as the establishment of systemic acquired resistance (Grant and Lamb 2006), and, therefore, plays a crucial role in plant defenses. The basal immune response to microbial pathogens requires the accumulation of SA (Fu and Dong 2013; Vlot et al. 2009). Results from a study of *Tobacco mosaic virus* have shown that direct cell-to-cell communication is a critical feature of the plant defense system, which can be regulated by SA through modifications of cell-to-cell permeability (Waigmann et al. 1994). The plasmodesmata

Yan Zhang and Xingfen Wang contributed equally to this work.

†Corresponding author: Zhiying Ma; E-mail: mzhy@hebau.edu.cn

*The *e*-Xtra logo stands for "electronic extra" and indicates that seven supplementary figures and four supplementary tables are published online.

© 2017 The American Phytopathological Society

(PD) allow for direct cytoplasmic connections and facilitate local molecular exchange among neighboring cells (Burch-Smith et al. 2011; Sevilem et al. 2013). Permeability of the PD structure can be altered during infections by microbial pathogens (Benitez-Alfonso et al. 2010; Heinlein 2002; Schoelz et al. 2011; Ueki and Citovsky 2011). This leads to changes in callose depositions at the PD (Lee et al. 2011).

No chemical control options for Verticillium wilt are available and cultural practices that can reduce disease severity are limited in effectiveness (El-Zik 1985; Mol et al. 1995; Zhang et al. 2013). Therefore, exploiting cotton genetic bases to improve Verticillium wilt resistance is the best and most sustainable strategy. Unfortunately, no source of heritable, highly effective resistance has been found in *G. hirsutum* (Wilhelm et al. 1974). By contrast, a source or sources of highly effective resistance have been identified in *G. barbadense*. However, it is unclear if the source of resistance is controlled by a single or a few dominant genes (Ma et al. 2000) and the trait has not been successfully transferred into *G. hirsutum* through conventional breeding techniques (Zhang et al. 2014). Transcriptome examinations of *G. barbadense* and *G. hirsutum* have demonstrated that Verticillium wilt resistance is a complex response (Sun et al. 2013; Xu et al. 2011). For example, defense genes are up- or down-regulated more quickly in resistant *G. barbadense* or more tolerant *G. hirsutum* cultivars than in susceptible cultivars of *G. hirsutum* (Sun et al. 2013). However, no definitive comparison of the physical or chemical responses that occur during the *V. dahliae*–host interaction has been made between closely related resistant and susceptible cotton species.

In this study, we found that the stronger intrinsic and induced physical and chemical barriers in *G. barbadense* than in *G. hirsutum* are associated with reduced colonization by *V. dahliae* and high resistance to the fungus.

RESULTS

Progression of *Verticillium dahliae* infection is restricted within *G. barbadense*.

To identify the mechanisms of *Verticillium dahliae* resistance in cotton, we used confocal laser scanning microscopy (CLSM) to examine conidial germination and hyphal colonization in the roots of *Gossypium barbadense* 'Pima90-53' and *G. hirsutum* 'CCRI8' for 72 h postinoculation (hpi). At 6 hpi, the conidia attached to the root surfaces of both species in general (Fig. 1A). By 12 hpi, several conidia had germinated, and germ tubes were emerging from one end of the conidium while secondary hyphae were growing (Fig. 1B and F). However, only a few conidia were found in the interior of the roots of *G. barbadense* (Fig. 1F). Differences between species were even more obvious at 48 hpi (Fig. 1D and H). By 72 hpi, *V. dahliae* had formed dense hyphal networks with a relatively large number of conidia-containing conidiophores in *G. hirsutum* roots, whereas *G. barbadense* roots had only small colonies with sparse hyphae (Supplementary Figs. S1 and S4). To support these qualitative observations, we quantified the number of conidia at 24 hpi and found that *G. barbadense* had significantly fewer conidia (Supplementary Fig. S2).

During additional experiments, surface-sterilized hypocotyl sections harvested from plants at 48 hpi were placed on potato dextrose agar (PDA) to examine the extent of *V. dahliae* colonization. Here, fewer colonies grew from *G. barbadense* (Supplementary Fig. S3). Moreover, quantitative (q)PCR showed that, at 21 days postinoculation (dpi), the fungal biomass in stem tissues was sixfold smaller for *G. barbadense* than for *G. hirsutum* (Fig. 2B). All of these observations suggested that the resistant *G. barbadense* supports less *V. dahliae* development.

Interspecific grafting experiments showed that type I–grafted plants (*G. hirsutum* on *G. barbadense* rootstock) exhibited only slight vascular browning on the rootstock half of the seedling but darker coloration on the scion half (Fig. 2C). The opposite was found with type II–grafted plants (*G. barbadense* on *G. hirsutum* rootstock). This demonstrated that the extent of infection was limited within the resistant *G. barbadense*. Together, these findings indicated that *V. dahliae* growth and biomass production were drastically restricted in the more resistant *G. barbadense*.

Plants of *G. barbadense* have stronger constitutive and induced physical and chemical defenses.

To identify factors in *G. barbadense* that are associated with reduced colonization by *V. dahliae*, we examined the levels of several important players in physical barriers, namely, lignin, phenolic acids, reactive oxygen species (ROS), and callose. The phloroglucinol-HCl (Wiesner) reaction, used to detect lignin, indicated that 96-hpi hypocotyl sections from infected plants of *G. barbadense* exhibited stronger red staining of xylem vessel walls and parenchyma cell walls than those from *G. hirsutum* (Fig. 3A). Quantitative analyses of 4-dpi seedlings showed that absolute constitutive levels of lignin in root and shoot of *G. barbadense* were 8.465 and 10.505 mg/g, respectively, which were higher than those of *G. hirsutum*. After inoculated with *V. dahliae*, the absolute levels of lignin, including constitutive and induced levels, in root and shoot of *G. barbadense* were 10.890 and 13.123 mg/g,

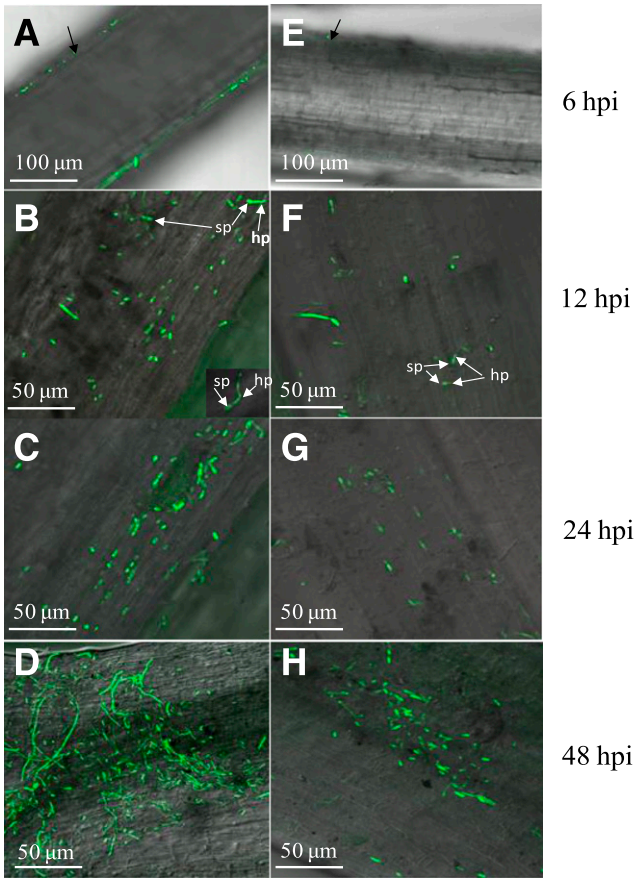

Fig. 1. Early stages of root colonization by green fluorescent protein–tagged isolate of *Verticillium dahliae* in **A** to **D,** *Gossypium barbadense* and **E** to **H,** *G. hirsutum*. Representative images of conidiospores were taken, at 6, 12, 24, and 48 h postinoculation (hpi), by laser scanning confocal microscope. Details of fungal structure were revealed via high magnification. hp = secondary hyphae, sp = conidiospore. Conidia-covered root of cotton at 6 hpi in *G. hirsutum* (A) and *G. barbadense* (E). Germ tubes emerging from one end of conidium (B, F), and resultant hyphae (C, G). Mass of hyphae in roots from *G. hirsutum* (D) and *G. barbadense* (H).

respectively, which were also higher than those of *G. hirsutum*. Furthermore, compared with preinoculation levels, total lignin increased by 25 and 23% in *G. barbadense* and by 39 and 28% in *G. hirsutum* stems and roots, respectively (Fig. 3B). However, absolute constitutive levels of lignin in *G. barbadense* were greater than induced levels in *G. hirsutum* for both tissues. This indicated that the higher absolute magnitude of lignin played stronger physical barriers in defense against *V. dahliae*.

Evaluation of the phenolic fractions revealed that autofluorescence accumulations induced by phenolic compounds in the stems were more intense postinoculation in *G. barbadense* than in *G. hirsutum* (Fig. 3C). Quantitative analysis via Folin-Ciocalteu assays indicated that the former also exhibited higher constitutive levels of soluble phenols in the stems (Fig. 3D).

Host cell walls can be strengthened directly by ROS, due to oxidative cross-linking of glycoprotein or the precursors of lignin and suberin polymers (Bradley et al. 1992; Hückelhoven 2007; Lamb and Dixon 1997). Both dichlorofluorescein-staining and enzyme-linked immunosorbent assays revealed that ROS accumulations were enhanced in the root tips of *G. barbadense* after inoculation, with the highest level at 24 hpi. By contrast, ROS accumulations peaked in *G. hirsutum* root tips and were not different than *G. barbadense* at 4 hpi. Overall, ROS levels were significantly higher in *G. barbadense* than in *G. hirsutum*, both before inoculation and at 24 hpi but not at 4 hpi (Fig. 4A and B).

Callose provides a physical barrier and structural reinforcement to restrict or retard pathogen attacks. Compared with our mock water control (distilled water used rather than inoculum), callose depositions were higher in both species postinoculation, as indicated by staining with aniline blue (Fig. 5A). In particular, callose levels in control and inoculated plants were approximately two and three times higher, respectively, for *G. barbadense* than for *G. hirsutum* (Fig. 5B). All of these experiments demonstrated that the two species differed in their response, suggesting that the stronger intrinsic defenses presented by *G. barbadense* are associated with its greater resistance to *V. dahliae*.

Levels of SA are higher in *G. barbadense* both pre- and postinoculation.

To assess whether SA levels change during *V. dahliae* infection, we used liquid chromatography–mass spectrometry to measure SA in root tissues before and after inoculation. Compared with the mock control, the total SA concentration in *G. barbadense* did not differ significantly at 12, 24, and 48 hpi but was sharply increased in *G. hirsutum*, peaking by approximately twofold at 24 hpi over the mock control before rapidly returning to the preinoculation level (Fig. 6). Despite this induced response, SA levels were similar to or significantly higher in *G. barbadense* than in *G. hirsutum* at each timepoint.

We also examined the relationship between SA levels and callose deposition in other cotton cultivars, namely, resistant *G. barbadense* 'Hai7124', tolerant *G. hirsutum* 'ND601', and the susceptible *G. hirsutum* 'Ji 11' and 'Han 208'. As expected, levels of both SA and callose for all four cultivars were higher in inoculated plants than in the mock controls (Fig. 7). Among these, resistant 'Hai7124' cotton exhibited significantly higher SA and callose levels in both control and inoculated plants. Although those levels were significantly lower in the tolerant 'ND601', they were significantly higher than in the two susceptible cultivars, except for SA in the mock control (Fig. 7). This similarity in the alterations of SA and callose deposition between *G. barbadense* and *G. hirsutum* both pre- and postinoculation suggested a consistent relationship between high levels of SA and callose.

SA helps confer *G. barbadense* resistance by inducing callose accumulations in the PD.

SA has an important role in basal defenses, resistance protein–mediated defenses, and systemic acquired resistance (Shah 2009; Wiermer et al. 2005). We found that, in the absence of infection, the endogenous SA content was significantly higher in *G. barbadense* than in *G. hirsutum* (Fig. 6). To explore how this might be associated with greater *Verticillium* resistance by *G. barbadense*, we used a virus-induced gene-silencing (VIGS) approach to silence *GbEDS1*, a key gene in the SA synthesis

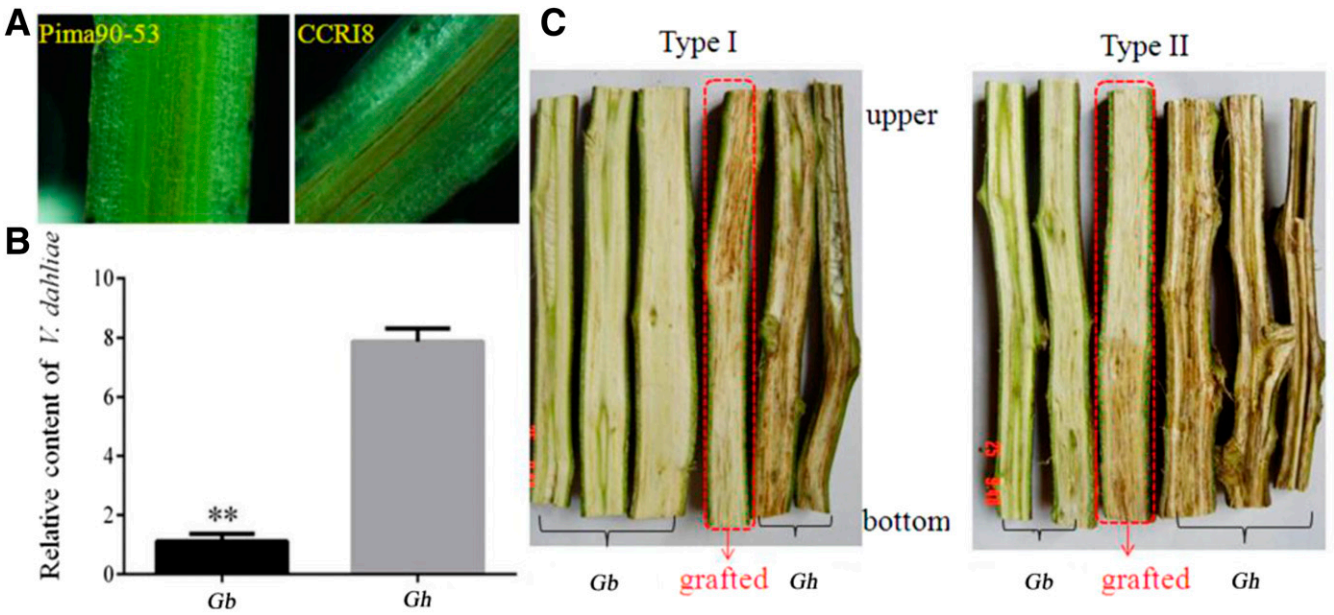

Fig. 2. Symptoms of Verticillium wilt in stems of cotton plants. **A,** At 21 days postinoculation, tissue-browning was rare in vascular bundles from *Gossypium barbadense* but severe in longitudinal sections from *G. hirsutum*. **B,** Fungal biomasses revealed by quantitative polymerase chain reaction assay. Normalized *Verticillium dahliae* infection coefficients were calculated as $IC = CT_{host}/CT_{pathogen}$. Error bar indicates standard deviation of three replicates; asterisks indicate values are significantly different at $P < 0.05$ (Tukey's test, $P < 0.01$). **C,** Difference in extent of browning for vascular bundles sampled from grafted tissues. Type I, using 'Pima90-53' as rootstock and 'CCRI8' as scion and type II, 'CCRI8' as rootstock and 'Pima90-53' as scion.

pathway in cotton (Su et al. 2014). At 14 days after *Agrobacterium* infiltration into *G. barbadense*, transcripts of *GbEDS1* were significantly reduced in VIGS vector (*Tobacco rattle virus* [TRV])::GbEDS1 plants compared with the TRV::00 control plants (Fig. 8E). Upon inoculation with *V. dahliae*, TRV::GbEDS1 plants showed more wilting and etiolated leaves, with greater incidence and severity of Verticillium wilt (Fig. 8, F, and G) when compared with the control (Fig. 8A). More fungal colonies were found in the roots of TRV::GbEDS1 plants (Fig. 8B and C).

We applied the high-pressure liquid chromatography tandem mass spectrometry (HPLC-MS/MS) method to investigate whether SA accumulation is altered after silencing *GbEDS1*. Compared with the control, SA levels in the roots of TRV::GbEDS1 plants were significantly lower. Comparisons of callose depositions between TRV::00 and TRV::GbEDS1 plants showed that callose densities were much lower in TRV::GbEDS1 plants at 48 hpi (Fig. 9C and D). These results indicated that the lower rate of callose deposition in TRV::GbEDS1 was associated with its impaired SA accumulation.

SA positively regulates PD-located protein expression, which in turn negatively controls PD permeability. To further connect SA production with callose deposition, we used Drop-ANd-See (DANS) assays and observed that permeability was significantly increased in the TRV::GbEDS1 plants when compared with that of the control (Fig. 9A and B). Real-time PCR analysis showed that transcripts of *GbPDLP1* and *GbPDLP6* (*PLASMODESMATA-LOCATED PROTEINs 1* and *6*), two cotton homologs of *PDLP5* from *Arabidopsis*, were significantly suppressed in the TRV::GbEDS1 plants (Fig. 9E). Taken together, these findings clearly showed that SA confers a part of resistance in *G. barbadense* by inducing callose accumulations.

V. dahliae–responsive transcript profiles differ between cotton species.

We compared the transcript profiles of *G. barbadense* and *G. hirsutum* in response to infection by *V. dahlia*, using RNA-Seq. A total of 1,272,047,736 tags that were at least 100 bp long were generated. Each sample was represented by about 5.0

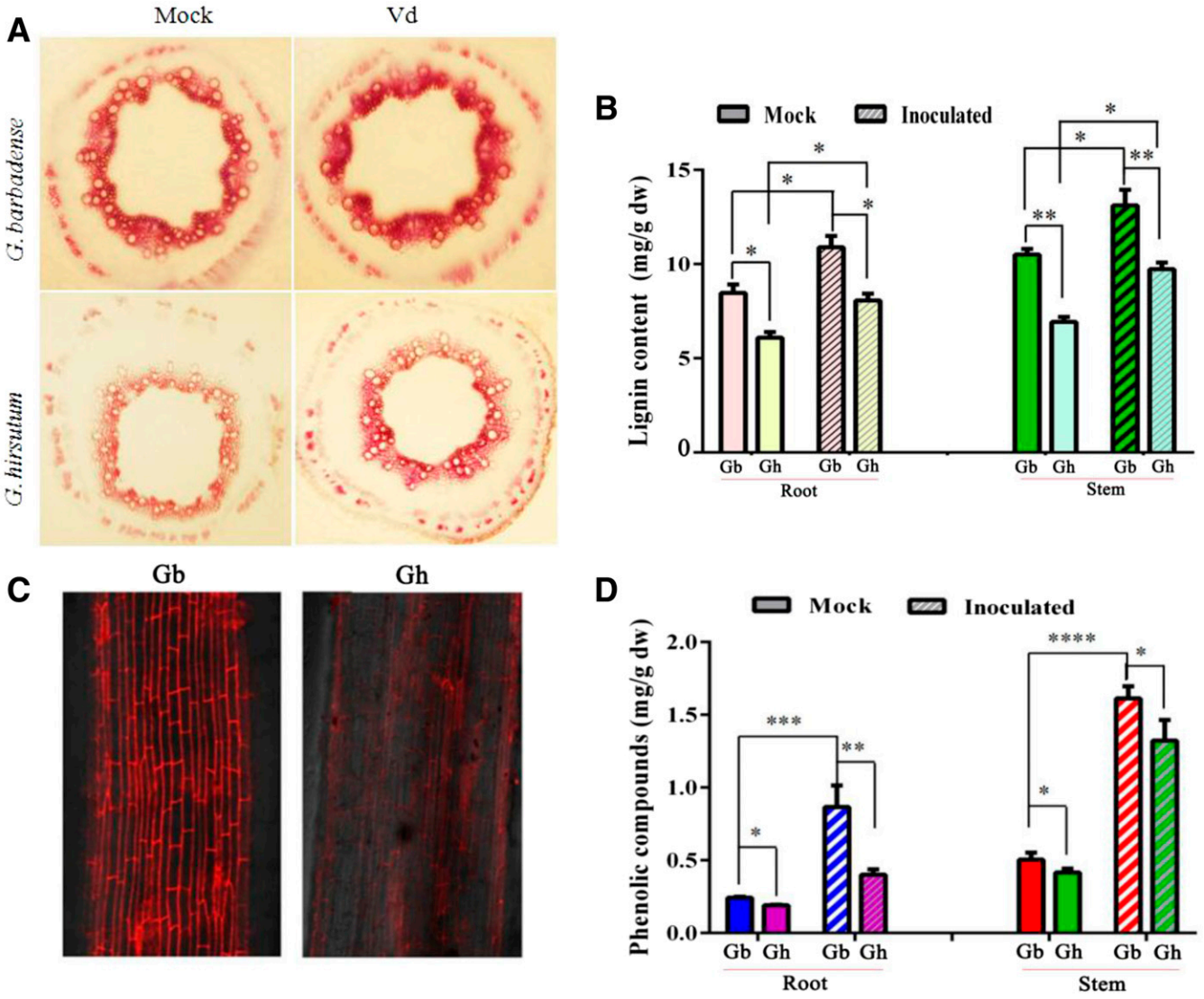

Fig. 3. Determination of lignin and phenolic compounds in cotton after inoculation by *Verticillium dahliae*. **A,** Light-microscope image of hypocotyl cross sections from *Gossypium barbadense* and *G. hirsutum* at 96 h postinoculation (hpi) after staining with phloroglucinol-HCl to detect lignin in mock control (inoculation with water only) and pathogen-inoculated plants. **B,** Lignin contents determined as lignin thioglycolic acid equivalents (milligrams per gram of dry weight). Quantifications were performed using alkaline lignin as standard. **C,** Fluorescence of phenolic compounds in roots at 96 hpi. Experiments were conducted five times ($n = 5$). Tissue was excited at 488 nm, and emitted light was examined between 577 and 624 nm. **D,** Content of soluble phenolic acids, measured through Folin-Ciocalteu assays. Phenolic fractions were normalized to the thioglycolic acid equivalent. Error bars indicate standard deviation; asterisks (****), values are significantly different at $P < 0.0001$, based on Tukey's tests.

million tags. We mapped sequences to the reference genome of *Gossypium_hirsutum*_v1.1 (CottonGen database) using BWA software (Li and Durbin 2009), allowing two-base mismatches. All tag information is summarized in Supplementary Table S1. Transcriptomic changes were measured via RNA-Seq in both species. Expression of 50,242 unigenes was detected in at least one of the 12 libraries of progressive timepoints that were sampled during this plant-microbe interaction. According to the K-means method from Genesis (Xu et al. 2011), all the responsive genes could be assigned to three groups based on their postinoculation patterns of expression (Supplementary Fig. S6). Group I contained four clusters of genes positively regulated during the cotton defense response. Group II genes, comprising three clusters, were negatively regulated, while those in group III showed complex expression patterns. The numbers of genes up- or downregulated at each sampling point are shown in Figure 10. As the time since inoculation increased, more genes were differentially expressed in each species, with more being downregulated than upregulated at each point. Fewer *V. dahliae*–responsive transcripts were detected in *G. barbadense* than in *G. hirsutum*. For the more resistant *G. barbadense*, the number of downregulated genes remained relatively constant between 12 and 48 hpi, while the number of upregulated genes rose over time. Analysis of functional gene enrichment presented 28 significantly enriched Kyoto Encyclopedia of Genes and Genomes pathways in *G. barbadense* versus 67 in *G. hirsutum* (Supplementary Fig. S7).

Investigation of the marker genes involved in systemic acquired resistance indicated that as many as 40 in the branch pathways for auxin, gibberellic acid, JA, and SA were induced in *G. hirsutum* versus only three in *G. barbadense* (Supplementary Table S2). Furthermore, the ACO and ACS genes, which are important in the ET pathway, were exclusively induced in the infected roots of *G. hirsutum*, as were genes that participate in the auxin and abscisic acid signaling pathways. Therefore, we can conclude that infection by *V. dahliae* induces systemic resistance in *G. hirsutum* but not in *G. barbadense*.

Pathways for major secondary metabolites are less influenced in *Verticillium*-infected *G. barbadense*.

We analyzed the transcript levels of 12 genes that are part of the flavonoid synthesis branch within the phenylpropanoid metabolic network and found that their expression rose steadily in *G. hirsutum* during the infection period. One of the most notable was the gene for flavonoid *O*-methyltransferase, for which transcript abundance was markedly increased from 0 to 12 hpi. Another gene, encoding caffeic acid *O*-methyltransferase (a key enzyme in the synthesis of the monolignols coniferyl and sinapyl alcohols), was also up-regulated. By contrast, only four of those genes were induced by pathogen inoculation in *G. barbadense* and only seven genes were constitutively expressed at a higher level than in *G. hirsutum* (Supplementary Table S3).

DISCUSSION

We have shown that *Gossypium barbadense* plants possess stronger constitutive and induced physical and chemical defenses than *G. hirsutum* plants do and that these defenses are associated with limited endophytic colonization by *V. dahliae* and reduced Verticillium wilt severity. Silencing a key gene in the SA pathway reduced the defenses of *G. barbadense*, leading to higher accumulations of fungal biomass and more severe wilt symptoms. These data provide new information about the resistance mechanism employed by *G. barbadense* against the fungus.

The development of CLSM has significantly broadened our knowledge of the colonization process of *V. dahliae* on host root (Zhao et al. 2014). Based on previous studies, the conidia were observed covered on either the main or lateral roots of *Arabidopsis* at 6 hpi. By 12 hpi, several conidia germinated, with the germ tubes emerging from one end of the conidium. By 24 hpi, many conidia had germinated and extended hyphae on the *Arabidopsis* root-hair zone. The penetration of *V. dahliae* hyphae into the roots was obvious by 48 hpi. By 72 hpi, hyphae across epidermal cells after penetration and internally grew

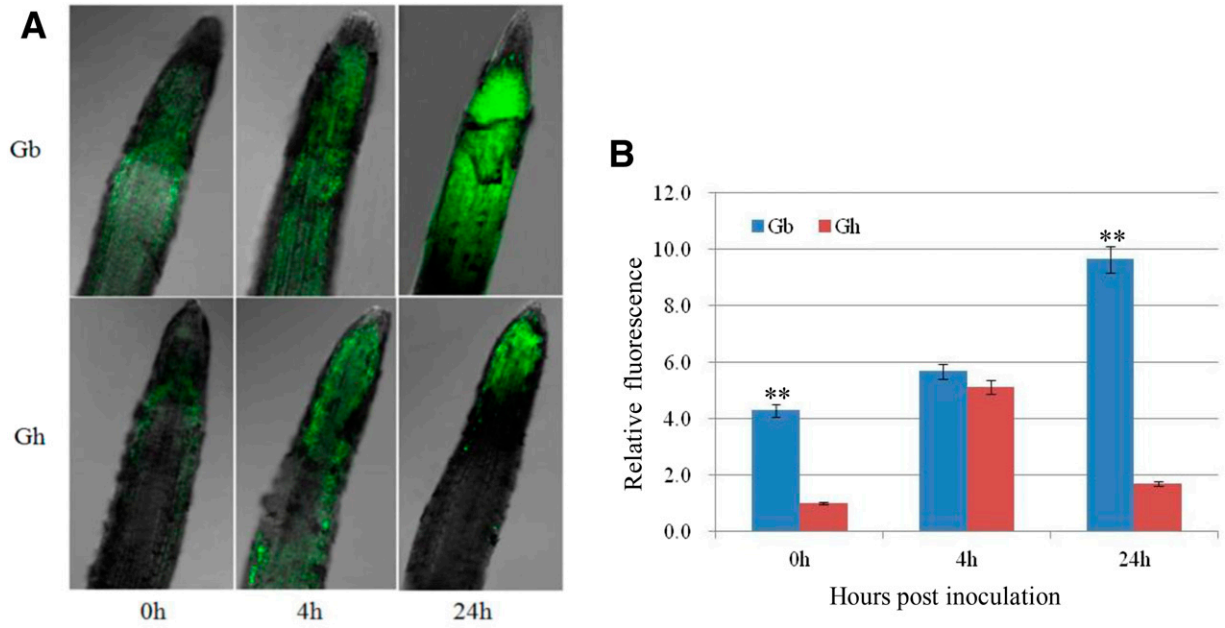

Fig. 4. Analysis of H_2O_2 accumulations in roots of *Gossypium barbadense* and *G. hirsutum* in response to *Verticillium dahliae* infection, as detected by dichlorofluorescein-staining and observed with fluorescence microscope. **A,** Postinoculation H_2O_2 production appears as green fluorescence in representative roots. **B,** Relative fluorescence intensity in root samples at various times postinoculation. Data are averages of three biological samples for each point. Error bars indicate standard deviations ($n = 3$); Asterisks indicate values are significantly different at $P < 0.001$ (Tukey's test, two asterisks (**), $P < 0.01$).

parallel along the longitudinal axis bidirectional (Zhao et al. 2014). All these studies guided our determination of the time-point for each sample, which coordinated with the disease cycles of cotton and *V. dahliae* interaction.

Compared with *G. hirsutum*, the progression of *V. dahliae* infection is restricted within *G. barbadense.* In general, the deposition of lignin and phenolics are important in resistance to vascular disease (Beckman 2000; Bradley et al. 1992; Eynck et al. 2009; Hückelhoven 2007; Keen 1992; Lamb and Dixon 1997; Xu et al. 2011). Along with callose, these factors provide a physical barrier to restrict barbaric colonization by pathogen. In this study, based on microscopic observation of the infection process and the grafting experiments, the extent of invasion by *V. dahliae* was restricted in *G. barbadense* and this mechanism was weaker in *G. hirsutum*. This phenomenon guided us to investigate the differences that were closely related to those physical barriers, including lignin, phenolic compounds, and callose. In general, constitutive levels and relative induced increase of defense were higher in *G. barbadense* than in *G. hirsutum*. However, this response was not consistent across factors. For example, absolute constitutive levels of lignin in *G. barbadense* were numerically greater than induced levels in *G. hirsutum* for both tissues. However, the percent increase of lignin is lower in *G. barbadense* than that in *G. hirsutum*; this result may be due to the fact that the constitutive response is more important for this defense mechanism in *G. barbadense* than that in *G. hirsutum*. And the induced response also takes part in the defense against the *V. dahliae* process.

In general, callose could provide a physical barrier or structural reinforcement to retard or restrict pathogen attacks (Jones and Dangl 2006; Schwessinger and Ronald 2012). Stress-induced callose synthesis is another important component of defense mechanisms (Ellinger et al. 2013; Jacobs et al. 2003). For example, in *Arabidopsis*, elevated depositions during the early phase of infection by the biotrophic fungi that cause powdery mildew lead to complete penetration resistance (Ellinger et al. 2014). In tomato (*Lycopersicon esculentum*) and *Arabidopsis*, plants challenged with the necrotrophic fungus *Botrytis cinerea* also accumulated callose formation (López-Cruz et al. 2017; Scalschi et al. 2015). All these studies indicate that callose deposition has an important role in defenses against biotrophic and necrotrophic fungi. However, no previous reports have elaborated on how callose production functions in defense against a hemibiotrophic fungus such as *V. dahlia*e. In this study, silencing of *GbEDS1* decreased SA level, thereby significantly increasing PD permeability, which then affected

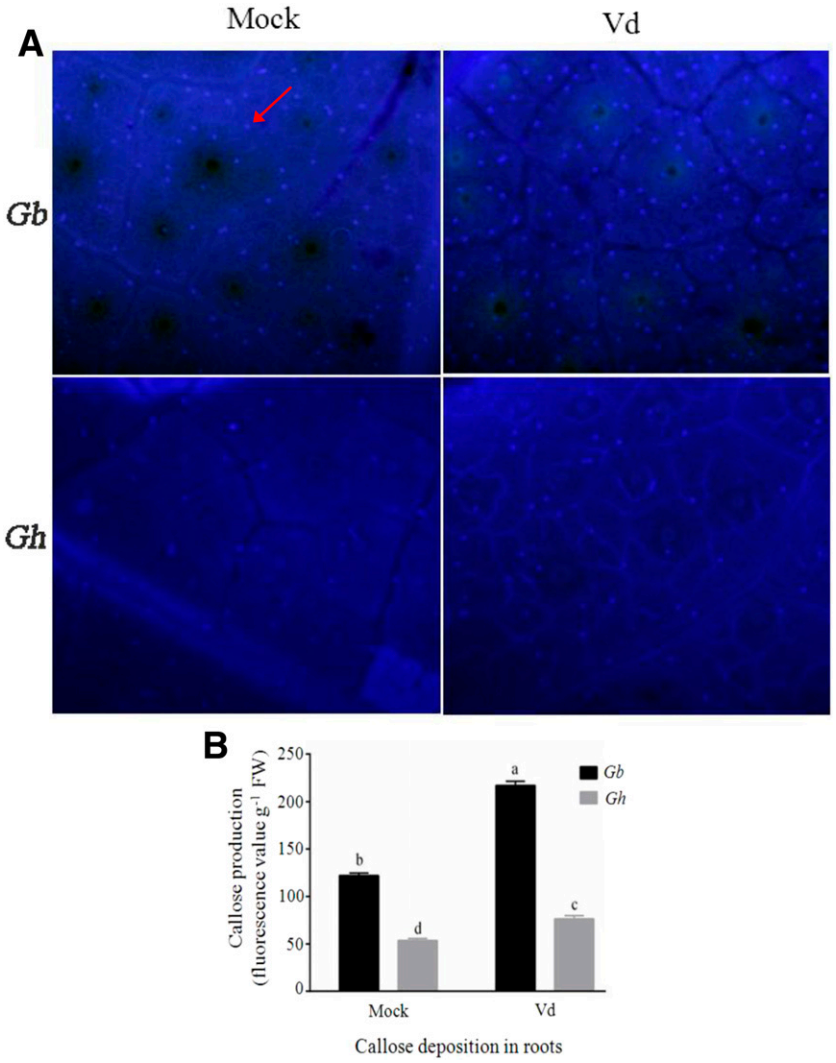

Fig. 5. Callose accumulations in leaves of *Gossypium barbadense* and *G. hirsutum* at 24 days postinoculation. **A,** Localization by aniline blue staining. Experiments were performed three times with $n > 10$ leaves (four areas per leaf). Arrows represent localization of deposition. **B,** Depositions in roots of pathogen-inoculated or mock-control plants. Error bars indicate standard deviations of three biological replicates; letters represent significant differences among treatments at $P < 0.001$ (Tukey's test).

the density of callose deposits. The callose levels were higher in *G. barbadense* than in *G. hirsutum*. Furthermore, callose depositon was much lower in TRV::GbEDS1 silent cotton plants, which displayed more serious disease than the mock plants. All these results may be associated with the high levels of callose deposition at the early infection stage in roots or leaves of *G. barbadense*. However, which part of infection process could be halted by the increased callose deposition should be studied in the future.

From earlier studies with other types of pathogens, researchers have reported that the expression of defense-responsive genes is often up- or downregulated. This usually occurs sooner in incompatible interactions (Mysore et al. 2002; Schenk et al. 2003; Tao et al. 2003; van Loon et al. 2006). We also found that the constitutive level and the timing of defense responses were associated with the extent of resistance to *V. dahliae*. For example, although *G. hirsutum* had a strong transcriptome response and fairly high SA levels, these perhaps occurred too late to have an important influence on pathogen resistance. By contrast, *G. barbadense* had high constitutive levels of SA. Although those levels during the infection period were similar between the tolerant *G. hirsutum* cultivar and the susceptible cultivars, the resistant and tolerant plants showed a much stronger induced response. This suggested that not only are high constitutive levels critical, but the size of the response also plays a role.

Microscopic observations combined with reisolation and quantification of *V. dahliae* in the cotton hypocotyls showed that *G. barbadense* tissues had fewer fungal hyphae in comparison with the *G. hirsutum* samples. Therefore, we deduced that this led to smaller modifications in levels of gene expression in *G. barbadense*, because the pathogen invasion was not as successful in that species. Even though *G. hirsutum* displayed massive reprogramming of its transcriptome, based on expression analysis, that effort failed to improve its resistance. For example, in this study, the percent increase of lignin is higher in *G. hirsutum* than that in *G. barbadense* and was coordinated with the large systemic increases in the expression of defense-related genes. It is possible that, in those more susceptible plants, the fungus spread systemically after penetration, thereby activating the same defense responses as shown by the resistant plants. In fact, large systemic increases in the expression of defense-related genes did not seem to protect *G. hirsutum* from the disease. This contrast is similar to the differences found between resistant and susceptible cultivars of tomato in response to *V. dahliae* attacks (Robb et al. 2012). All the above results may be due to the constitutive response being more important for this defense mechanism in *G. barbadense* than that in *G. hirsutum*.

If the first defense mechanisms prove ineffective and the stress persists, levels of some hormones, e.g., auxin and ET, can rise, causing a cascade of secondary metabolic and growth responses (Eynck et al. 2009). We found here that many more genes associated with the auxin or ET pathways were induced by *V. dahliae* in *G. hirsutum*, again implying that the earlier phases of the defense response had failed in that species. The discrepancy in the strength of the transcriptome response versus the degree of plant resistance noted here was of interest to us. Based on previous reports (Schenk et al. 2003; van Loon et al. 2006), we hypothesized that the highly resistant *G. barbadense* would show a much stronger *V. dahliae*–induced transcriptional response. Instead, we detected dramatic changes in the expression of thousands of genes in the susceptible *G. hirsutum* but fewer and weaker alterations in expression in the resistant *G. barbadense*. This is consistent with findings described by Robb et al. (2012), in which susceptible tomato showed strongly altered expression of many defense-related genes after plants were inoculated with *V. dahliae*, even though the systemic responses were not always effective. By contrast, genes in the resistant tomato were not generally up- or down-regulated significantly, even though such plants had successfully resisted those pathogen attacks. Fung et al. (2008) investigated the relationship between various *Vitis* spp. and the fungi responsible for powdery mildew and found only three mildew-responsive transcripts in resistant *V. aestivalis* but 625 in susceptible *V. vinifera* (Fung et al. 2008).

At 12 and 24 hpi, the rates of SA increase in infected cotton roots were significantly lower in *G. barbadense* than in *G. hirsutum*, even though that hormone was maintained at

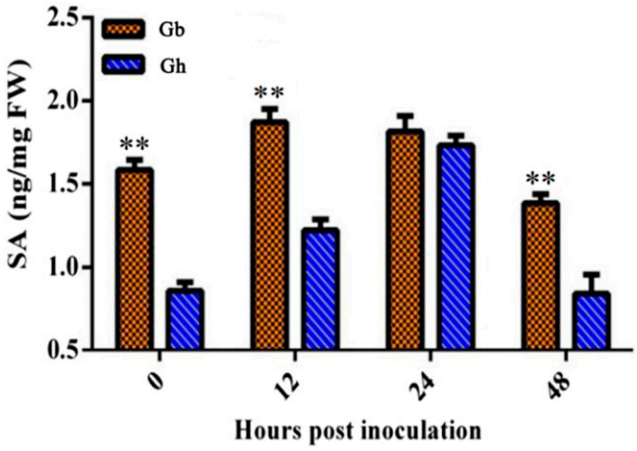

Fig. 6. Endogenous levels of total salicylic acid (SA) accumulated in *Gossypium barbadense* (diagonal pattern) and *G. hirsutum* (hatched pattern) measured at 12, 24, and 48 h postinoculation. Data are averages of three biological samples for each timepoint. Error bars indicate standard deviations ($n = 3$); two asterisks (**), values are significantly different at $P < 0.01$ (Tukey's test).

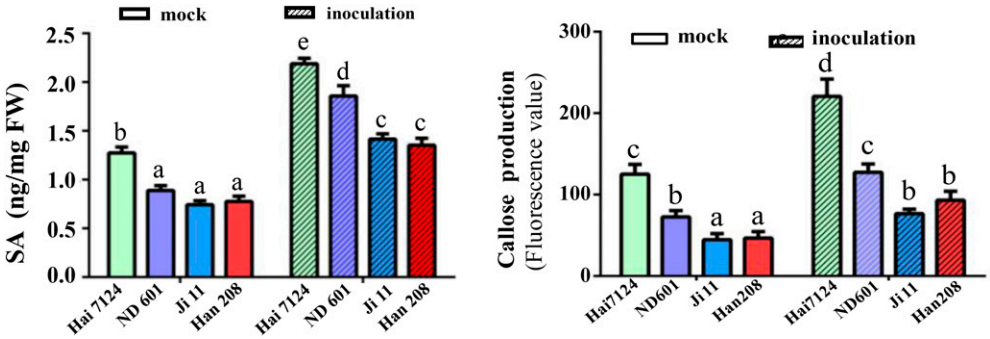

Fig. 7. Endogenous levels of total salicylic acid (SA) accumulated and callose depositions in several cotton cultivars at 24 h postinoculation. Data are averages of three biological samples for each timepoint. Error bars indicate standard deviations ($n = 3$); Different letters indicate significant differences (Tukey's test; $P < 0.05$).

higher levels in the former. However, the transcriptome of defense response–related genes in *G. hirsutum* was much more dramatically changed compared with those in *G. barbadense*. It is possible that *G. barbadense* is more efficient in its response or that *G. hirsutum* activates additional pathways because the disease either progresses further in that species or greater fungal biomass accumulates there. Additional experiments will be needed to answer these questions. Combined with the detected results, we found that the levels of physical barrier were more or less higher in *G. barbadense* than those in *G. hirsutum*. Are there fitness costs for these high levels in *G. barbadense* in the absence of pathogen? More experiments should be carried out to make the answer clear.

In conclusion, we compared the differences between species regarding their corresponding levels of lignin, phenolic compounds, ROS, callose, and SA as part of their physical barrier to pathogen infections. Here, the intrinsic defense was stronger in *G. barbadense*. By improving our understanding of the molecular

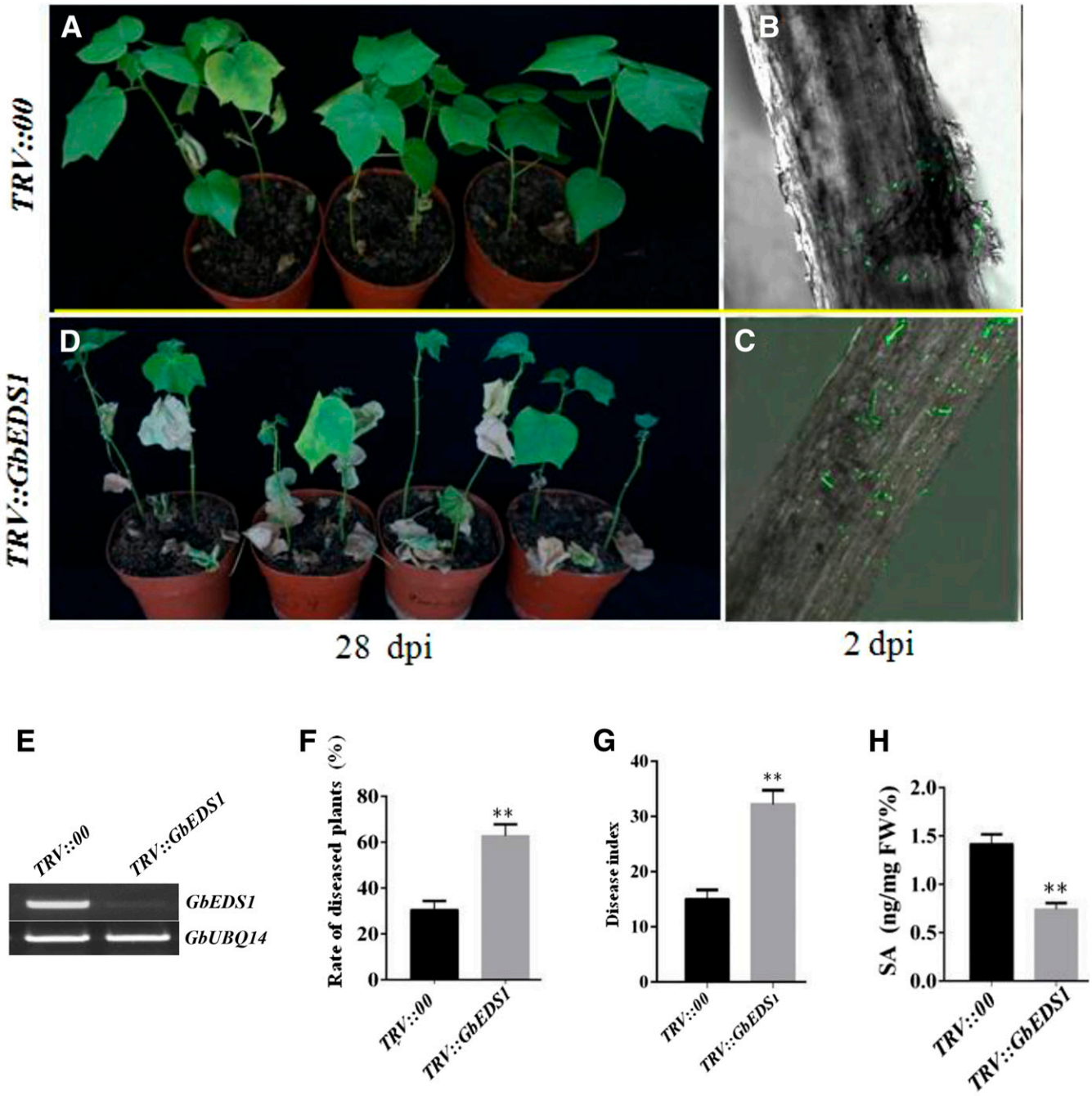

Fig. 8. Effects of silencing *GbEDS1* on cotton susceptibility to *Verticillium dahliae*. Ten-day-old *Gossypium barbadense* seedlings were hand-infiltrated with an *Agrobacterium*-carrying target gene in virus-induced gene silencing vector. Two weeks after infiltration, seedlings were dip-inoculated. **A,** Response of TRV::00 and **D,** TRV::EDS1 plants to pathogen at 28 days postinoculation (dpi). **B,** Early stages of root colonization by green fluorescent protein–tagged isolate of *V. dahliae* in TRV::00 and **E,** TRV::EDS1 at 2 dpi. **C,** Progression of infection in basal portion of stems from *G. barbadense* and **F,** *G. hirsutum*. Photos were taken at 5 dpi. **G,** Semiquantitative reverse transcription-polymerase chain reaction analysis of *GbEDS1* transcripts in control and silencing seedlings. **H,** Frequency of diseased plants and calculation of disease index for TRV::00 and TRV::GbEDS1 plants inoculated via the root-dipping method. Assessments were made 5 days after plants began presenting symptoms. Error bars represent standard deviations of three biological replicates ($n \geq 30$); asterisks (**) indicate values are significantly different at $P < 0.01$, based on Tukey's test.

mechanism against *V. dahliae*, we should be able to develop a genetics program to enhance practical disease resistance in cotton.

MATERIALS AND METHODS

Plant growth, pathogen inoculation, and separation.

Seeds of *Gossypium barbadense* cv. Pima90-53 and *G. hirsutum* cv. CCRI8 cotton were surface-disinfected in 0.5% sodium hypochlorite (NaOCl) for 5 min and were then washed five times with sterile distilled water. After they were transferred to wet, sterile towels in petri dishes (90 mm diameter), they were placed in a biochemical incubator at room temperature (RT) for 48 h, until they germinated. Any seeds presenting internal fungal contamination were discarded. Seedlings of similar size were selected and cultivated in dishes containing sterile vermiculite under the following growth chamber conditions: 16-h photoperiod, 30 ± 2°C (day) and 25 ± 2°C (night), and 75% relative humidity. Hoagland's nutrient solution was added to the dishes every 2 days.

For our inoculum source, we isolated the highly aggressive, defoliating *Verticillium dahliae* T5 from field-grown upland cotton plants that showed typical symptoms of infection. The green fluorescent protein–tagged *V. dahliae* strain Vd-gfp77 was used in our observations of the colonization process during the experimental period. Its pathogenicity on cotton is related to that of the wild-type isolate Vd991 (Xu et al. 2013). To initiate conidia production, we subcultured the T5 strain from PDA plates onto Czapek's medium (2 g of $NaNO_3$, 1 g of K_2HPO_4, 1 g of $MgSO_4{\cdot}7H_2O$, 1 g of KCl, 2 mg of $FeSO_4{\cdot}7H_2O$, and 30 g of sucrose per liter). After incubation at 25°C for 3 to 5 days, the concentration of conidia was adjusted with deionized water to approximately 10^7 ml^{-1}.

Seedlings of both species were removed from the vermiculite and were dip-infected with liquid containing either T5 or Vd-gfp77. Samples of seedlings inoculated with the T5 strain were used for RNA extraction, while those seedlings inoculated with the gfp77 strain were used for observing the infection progress.

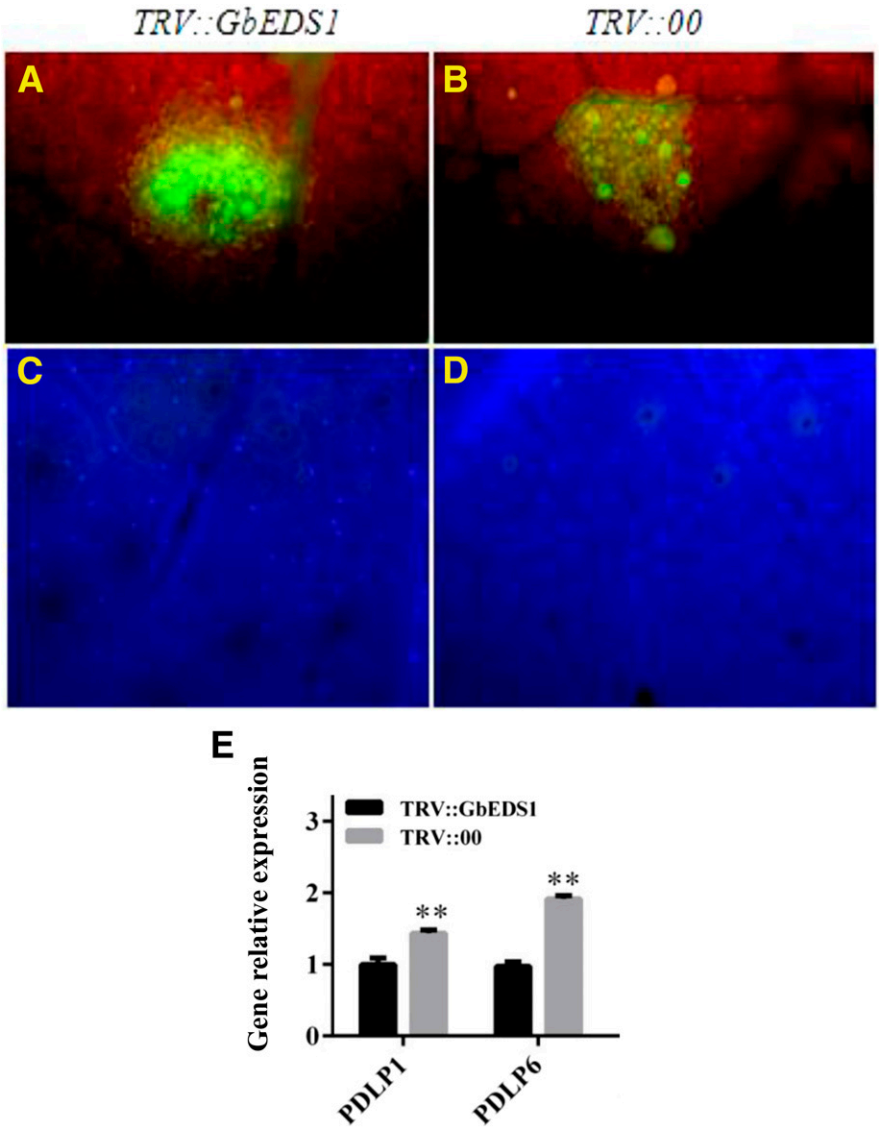

Fig. 9. Regulation of plasmodesmata (PD) closure and callose accumulation by salicylic acid. **A** and **B,** Comparison of PD permeabilities in TRV::GbEDS1 and TRV::00 plants based on drop-and-see assays. Confocal images show representative carboxyfluorescein diacetate movement on abaxial leaf surfaces. Green coloration indicates extent of dye diffusion. **C** and **D,** Localization of callose deposition in leaves at 24 h postinoculation, as revealed by aniline blue staining. Experiments were performed three times (n = 4 leaves). **E,** Quantitative polymerase chain reaction showing relative expression of PD-located protein genes. Three technical replicates were analyzed. Error bar represents standard deviation for three independent experiments; asterisks (**) indicate values are significantly different at $P < 0.01$, based on Tukey's test.

They were then incubated at 25°C under a 16-h photoperiod, and their roots were harvested at 6, 12, 24, 36, and 48 hpi. Mock control seedlings were treated with sterile distilled water. All root samples were stored at –80°C prior to the RNA extractions. For reisolating *V. dahliae* from infected seedlings, surface-sterilized hypocotyl sections were placed on the PDA medium and the extent of colonization was defined by the number of stem sections from which the fungus grew.

Microscopic observations.

Roots from three to five plants per species were sampled at 0, 6, 12, 24, 36, 48, and 72 hpi, as well as at 96 hpi. The soil was gently washed from the tissues, which were then sectioned longitudinally by hand with a double-edged platinum razor blade into 1-to 2-mm-thick slices or, in the case of fine roots, mounted whole. The CLSM settings needed for monitoring the process of colonization by green flujorescent protein (GFP)-tagged *V. dahliae* were based on those described by Vallad and Subbarao (2008). Briefly, we used a Nikon compound microscope with filter blocks for GFP (450 to 490 nm excitation, 590 nm longpass emission) coupled to an MRC1024 Bio-Rad Confocal System (Bio-Rad). All settings were optimized for GFP with excitation via a 488 argon laser, detection of emitted light at 522 DF32, and autofluorescence detection at 680 DF32 through a 598/40 center bandpass filter. Digital images acquired from individual channels were merged.

Isolation and quantification of *V. dahliae* DNA in cotton hypocotyls.

Five inoculated and five mock-control plants were harvested for real-time qPCR analyses at 21 dpi. Samples, approximately 5 cm long, were excised from the hypocotyl (below the cotyledon node). Roots were not included in this analysis because it was impossible to distinguish between the fungal biomass within the roots and the fungus attached to the root surface. Both DNA isolation and PCR analysis were performed as described previously (Pasche et al. 2013; Valsesia et al. 2005). Cotton *GhUBQ14* (GenBank accession number DW505546) was used to normalize quantification while the trypsin protease gene *VTP1* (GenBank accession number AY354459.1) of the pathogen was used as the detected target (Dobinson et al. 2004). All qPCR assays were conducted on a LightCycler real time PCR system (Roche), using SYBR green I for the detection of PCR products. Pure host DNA and pathogen DNA were balance-mixed and were then serially diluted in sterile water (1:2, 1:4, 1:8, 1:16 1:32, 1:32, and 1:64) to investigate the amplification efficiencies of *VTP1* (pathogen) and *GhUBQ14* (host). Each reaction was performed in a final volume of 20 µl that contained 10 µl of SYBR green PCR master mix (Applied Biosystems), 250 nM for each primer, and 50 ng of template. No-template reactions were included as negative controls for each set of primers. All primers are listed in Supplementary Table S4. The thermal cycling conditions were 94°C for 5 min, followed by 40 cycles for 94°C for 10 s, 55°C for 10 s, and 72°C for 15 s, with fluorescence detection at the end of each cycle. The amplification of a single product per reaction was confirmed by melting curve analysis. All reactions were performed in technical triplicates. As shown in Supplementary Figure S5, the amplification efficiency for each detected primer was more than 99%. Normalized *V. dahliae* infection values for leaf tissue were obtained by dividing the cotton cycle threshold (CT) value by the fungus CT value ($CT_{host}/CT_{pathogen}$). This ratio represented the infection coefficient, with a high ratio corresponding to an elevated degree of infection (Valsesia et al. 2005).

Grafting experiments.

Grafted plants were obtained by placing either *G. hirsutum* onto *G. barbadense* rootstocks (type I) or *G. barbadense* onto *G. hirsutum* rootstocks (type II) in the field disease nursery. Seedlings with at least one true leaf each were grafted according to the method of Wang et al. (2007). To facilitate the union of rootstock and scion, seedlings were placed in a shaded plastic tunnel (approximately 28°C) with a humidifier to maintain 100% humidity. After 7 to 10 days, they were acclimated to natural environmental conditions for 7 days. Their management practices followed those of other field-grown plants. All grafted and mock-control plants were treated at the disease nursery in the field. To compare colonization by *V. dahliae* within *G. barbadense* or *G. hirsutum*, we examined stems at the end of the growing season. Plants from each treatment were harvested and longitudinally sectioned, using three replicates per grafting type.

Extraction of phenolic compounds.

Pathogen-inoculated and mock-treated plants (10 each) of both species were harvested and divided into root and hypocotyl portions. Up to 200 mg of tissue was extracted for 1 h at RT in 1.5 ml of 80% aqueous methanol, then, centrifuged (13,000 × *g*) for 10 min at 4°C. The supernatant representing each category of tissue type, treatment, and species was retained and the process was repeated. After extraction, all supernatants

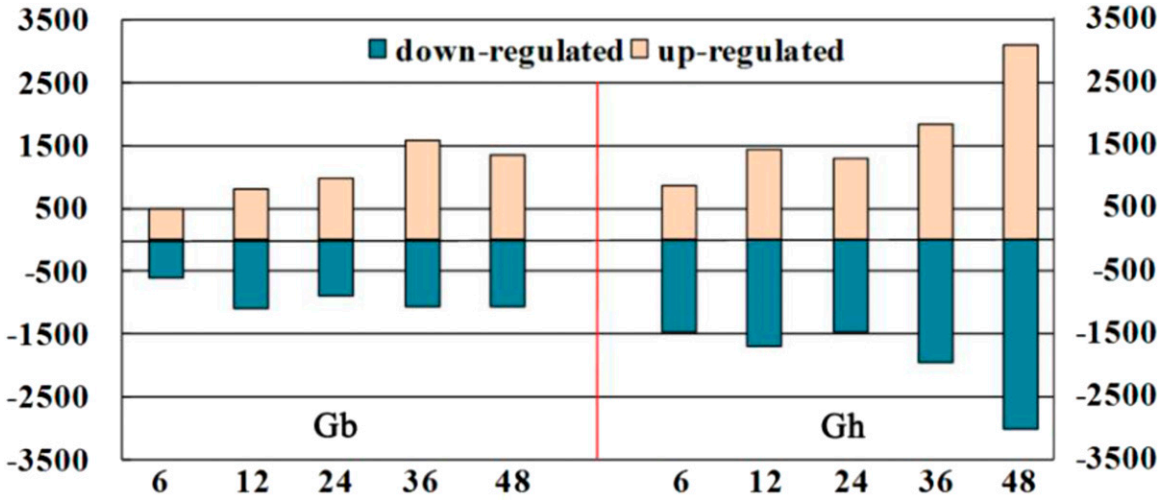

Fig. 10. Number of differentially expressed genes at 6, 12, 24, 36, and 48 h postinoculation in *Gossypium barbadense* and *G. hirsutum*. Genes were filtered with a cut-off of $P < 0.001$ and absolute value of $\log_2$Ratio >1, based on a false discovery rate <0.05.

within the same category were combined and were used for a modified version of the Folin-Ciocalteu assay (Eynck et al. 2009). Briefly, 200 µl of extract was added to 200 µl of distilled water and 400 µl of Folin-Ciocalteu reagent. After incubation for 3 min at RT, 400 µl of 1 M Na_2CO_3 was added. Following further incubation on a rotary shaker for 45 min at RT, absorbance of the samples was measured at 725 nm. Tannin was used as an external standard, and the total content of soluble phenolic compounds was reported as tannic acid equivalents based on a calibration curve. We also used autofluorescence and CLSM to visualize the accumulations of phenolic compounds according to the method of von Röpenack et al. (1998).

Extraction and quantification of lignin.

After the bound phenolic compounds were extracted, the cell walls from the sample remnants were washed sequentially with 80% methanol, distilled water, and acetone, followed by drying. The pellets were dissolved in 2 M HCl and thioglycolic acid, were then incubated for 4 h at 95°C with continuous shaking, and were centrifuged for 5 min (13,000 × *g*, 4°C). After the supernatant was discarded, the pellet remains were washed twice with water and were incubated in 0.5 M NaOH for 12 h. Following centrifugation, the supernatant was collected and 0.5 M NaOH was added to the residues for repeated incubations. Pooled supernatants were acidified with 32% HCl and were precipitated as a lignothioglycolic acid complex. The samples were incubated for 4 h at 4°C and were centrifuged, and the lignin pellets were resuspended in 0.5 M NaOH. The lignin content was determined at 340 nm. Quantification was performed according to a calibration curve obtained for alkaline lignin.

Histochemical analyses.

Hypocotyl samples were taken at 96 hpi from 10 pathogen-inoculated and 10 control plants of each species. For histochemical analysis, 2-cm-long segments were excised and preserved in a mixture of acetic acid/formalin/ethanol (5:5:90, vol/vol/vol). Tissues were transverse cross-sectioned on a vibration microtome (VT 1000M; Leica). Lignin histochemistry was examined using Wiesner reagent (Pomar et al. 2004). The cross sections were incubated for 10 min in either a phloroglucinol solution (2% in 95% ethanol) or 95% ethanol (staining control) and were then treated with 18% HCl for 5 min and directly observed, under bright-field conditions, with a fluorescence microscope (DM2500; Leica).

Cytochemical detection of hydrogen peroxide.

Seedlings in which the first true leaf was beginning to emerge were inoculated with *V. dahliae* by the dip method (Zhang et al. 2013). Fresh root tips were harvested at 0, 4, and 24 hpi, taking three biological replicates per timepoint. The stress-induced production of hydrogen peroxide (H_2O_2) was monitored at the subcellular level using dichlorodihydrofluorescein diacetate (DCFH-DA) (Sigma-Aldrich) for localization (Mai et al. 2013). Briefly, small segments of roots were excised 2 to 5 mm from the tips and were incubated for 1 h in 20 mM phosphate buffer (pH 6.0) to remove any ROS that may have been generated during the stripping process. The samples were then exposed for 30 min to stressors such as 200 mM NaCl, 10 mM potassium phosphate buffer (pH 3.0), or 50 mM H_2O_2. After those treatments, the root tips were floated on a solution of 50 µM DCFH-DA for 10 min and were then observed with a fluorescence microscope (excitation: 450 ± 490 nm, barrier: 520 ± 560 nm) (FV500, Olympus;). Using the quick selection and magic wand tools in Photoshop CS6 (Adobe), the quantity of every portion of the fluorescence signal was measured with ImageJ software, version 1.48u (National Institutes of Health).

Quantification of SA.

Seedlings showing the beginning of true leaves were inoculated with *V. dahliae* by the dip method. Fresh root samples were harvested at 0, 12, 24, and 48 hpi (three biological replicates per timepoint). The extraction and measurement of endogenous SA were performed as described by Gao et al. (2013). Three replicates of each frozen sample (approximately 100 mg per replicate) were ground to a fine powder in liquid nitrogen and were mixed with 750 µl of cold extraction buffer (methanol/water:/acetic acid, 80:19:1, vool/vol/vol). After shaking for 16 h at 4°C in the dark, the supernatants were collected and were then passed through a syringe-facilitated 13-mm-diameter nylon filter with a pore size of 0.22 µm (Nylon 66; Jin Teng Experiment Equipment Co. Ltd.). Filtrates were dried using nitrogen gas at RT and were then dissolved in 200 µl of methanol. For quantification, an aliquot of dissolved sample was further diluted 100 times, using methanol because cotton plants contain high levels of SA. Supernatants were analyzed via HPLC-MS/MS (1200L LC-MS system; Varian).

Visualization and measurement of callose.

Callose depositions were visualized by aniline blue staining, as described by Schenk et al. (2014). Each leaf sample was first destained in 1:3 acetic acid/ethanol for 24 h and were then stained with 0.01% aniline blue in 150 mM K_2POH_4 (pH 9.5). Stained tissues were examined under a fluorescence microscope (Eclipse E600, Nikon) that was equipped with a G-2A filter block, 510- to 560-nm excitation filter, 575-nm dichroic mirror, and 590-nm barrier filter.

The callose content in the roots was measured according to the method of Jones et al. (2006). Briefly, root tips (50 mg) were cut and were immediately fixed in 98% ethanol overnight. After the ethanol was discarded, the roots were homogenized in 400 µl of 1 M NaOH, with a small pestle. The samples were heated at 80°C for 15 min before being centrifuged at 1,000 × *g* for 10 min. Afterward, 71 µl of the supernatant was mixed with 142 µl of 0.1% aniline blue, 75 µl of 1 M HCl, and 210 µl of 1 M glycine-NaOH buffer (pH 9.5). This mixture was then heated (50°C, 20 min) and left to cool before its callose content was determined on a fluorescence spectrophotometer (RF5301; Shimadzu), under conditions of 400 nm excitation, 510 nm emission, and a 10-nm slit width.

RNA extraction and transcriptome analysis.

Total RNA was isolated from cotton roots using an RNeasy kit (Qiagen). The RNA integrity was determined with an Agilent Bio Analyzer 2100. Only those samples with integrity values >7 were used for RNA-Seq. The transcript abundance between *V. dahliae*–inoculated and mock-control plants of both species was compared at 0, 6, 12, 24, 36, and 48 hpi. Differentially expressed genes were filtered with a cut-off of $P < 0.001$ and an absolute value of $\log_2$ratio > 1, based on a false discovery rate (FDR) < 0.05 (Audic and Claverie 1997). The K-means method was used for cluster analysis of the gene expression profiles (Xu et al. 2011). Furthermore, marker genes involved in pathways for hormone signaling, cell-wall synthesis, and metabolism were investigated based on the results of our transcriptomic analysis.

VIGS in cotton followed by pathogen inoculation.

The VIGS vectors and *Agrobacterium tumefaciens* for VIGS were prepared as described by Gao et al. (2011). Inserts to generate TRV::GbEDS1 and the positive control TRV::GbCLA1 (cloroplastos alterados 1) were amplified from the cDNA of *G. barbadense*. The PCR fragments were digested with *Xba*I and *Sac*I and were then ligated into the TRV::00 plasmid. Constructs were transformed into *A. tumefaciens* GV3101 by electroporation. The TRV vectors were agroinfiltrated into the cotyledons of 7-day-old *G. barbadense* seedlings. Afterward, the plants

were grown in a controlled environment chamber (25°C, 16-h photoperiod). Because a bleached-leaf phenotype appeared in the TRV::GbCLA1 plants at 14 days after infiltration, we selected that as the best time to inoculate the seedlings with GFP-tagged *V. dahliae*. The frequency of diseased plants and disease index (DI) scores were obtained for at least 30 plants per treatment per species and ratings were repeated at least three times. The DI was determined according to the method of Ma et al. (2000), with scores assigned along a symptom scale ranging from 0 (none) to 4 (severe). This index was used to reflect the status of infection for a population rather than individual plants, with a lower DI value indicating greater disease resistance.

Real-time PCR analysis.

For selected genes, differential expression was verified by qPCR. This analysis was performed with three biological replicates and three technical replicates. For each sample, cDNA was serially diluted in sterile water (1:2, 1:4, 1:8, 1:16 1:32, 1:32, and 1:64) to investigate the amplification efficiencies of the primers. The qPCR procedure involved 20-µl samples run in three technical replicates on a LightCycler real time PCR system (Roche) that used 2 µl of first-strand cDNA and SYBR green PCR master mix (Takara). Amplification conditions included the following: one cycle at 94°C for 15 s; then 40 cycles at 94°C for 10 s, 59°C for 10 s, and 72°C for 15 s. The amplification of a single product per reaction was confirmed by melting curve analysis. No-template reactions were included as negative controls for each set of primers. *GhUBQ14* served as the reference gene to normalize the total amount of cDNA in each reaction (Artico et al. 2010). Relative fold-differences in mRNA abundance were defined by the mathematical model described by Livak and Schmittgen (2001).

DANS assay.

We performed DANS dye-loading assays with second leaves harvested from 2-week-old plants. Briefly, 1 ml of 1 mM 5(6)-carboxyfluorescein diacetate (Sigma-Aldrich) was loaded on the adaxial side of an intact target leaf and incubation was allowed for 5 min before the dye was withdrawn. Afterward, the leaf was removed from the plant and was mounted on a glass slide for confocal imaging under a Fluar ×5/0.25 objective lens, using 488-nm laser excitation with a 505- to 550-nm band-pass emission filter (Wang et al. 2013). The extent of dye diffusion was reflected by the diameter of the diffusion area with respect to the fluorescent intensity.

ACKNOWLEDGMENTS

We are grateful to Y. Liu (College of Life Science, Tsinghua University, Beijing, China) and or X. Dai (Chinese Academy of Agricultural Sciences) for providing the *Tobacco rattle virus*-induced gene silencing vectors and green fluorescent protein–tagged *V. dahliae* Vd-gfp77, respectively. This work was financially supported by the Natural Science Foundation of Hebei Province (C2017204011), Young Talents Support Program of Hebei Province.

LITERATURE CITED

Artico, S., Nardeli, S. M., Brilhante, O., Grossi-de-Sa, M. F., and Alves-Ferreira, M. 2010. Identification and evaluation of new reference genes in *Gossypium hirsutum* for accurate normalization of real-time quantitative RT-PCR data. BMC Plant Biol. 10:49.

Audic, S., and Claverie, J. M. 1997. The significance of digital gene expression profiles. Genome Res. 7:986-995.

Beckman, C. H. 2000. Phenolic-storing cells: Keys to programmed cell death and periderm formation in wilt disease resistance and in general defense responses in plants? Physiol. Mol. Plant Pathol. 57:101-110.

Benitez-Alfonso, Y., Faulkner, C., Ritzenthaler, C., and Maule, A. J. 2010. Plasmodesmata: Gateways to local and systemic virus infection. Mol. Plant-Microbe Interact 23:1403-1412.

Bradley, D. J., Kjellborm, P., and Lamb, C. J. 1992. Elicitor- and wound-induced oxidative cross-linking of a proline-rich cell wall protein: A novel, rapid defense response. Cell 70:21-30.

Burch-Smith, T. M., Stonebloom, S., Xu, M., and Zambryski, P. C. 2011. Plasmodesmata during development: Re-examination of the importance of primary, secondary, and branched plasmodesmata structure versus function. Protoplasma 248:61-74.

Cai, Y. F., He, X. H., Mo, J. C., Sun, Q., Yang, J. P., and Liu, J. G. 2009. Molecular research and genetic engineering of resistance to Verticillium wilt in cotton: A review. Afr. J. Biotechnol. 8:7363-7372.

Chen, P., Lee, B., and Robb, J. 2004. Tolerance to a non-host isolate of *Verticillium dahliae* in tomato. Physiol. Mol. Plant Pathol. 64:283-291.

Dobinson, K. F., Grant, S. J., and Kang, S. 2004. Cloning and targeted disruption, via *Agrobacterium tumefaciens*-mediated transformation, of a trypsin protease gene from the vascular wilt fungus *Verticillium dahliae*. Curr. Genet. 45:104-110.

Durrant, W. E., and Dong, X. 2004. Systemic acquired resistance. Annu. Rev. Phytopathol. 42:185-209.

Eggert, D., Naumann, M., Reimer, R., and Voigt, C. A. 2014. Nanoscale glucan polymer network causes pathogen resistance. Sci. Rep. 4:4159.

El-Zik, K. M. 1985. Integrated control of Verticillium wilt of cotton. Plant Dis. 69:1025-1032.

Ellinger, D., Glöckner, A., Koch, J., Naumann, M., Stürtz, V., Schütt, K., Manisseri, C., Somerville, S. C., and Voigt, C. A. 2014. Interaction of the *Arabidopsis* GTPase RabA4c with its effector PMR4 results in complete penetration resistance to powdery mildew. Plant Cell 26:3185-3200.

Ellinger, D., Naumann, M., Falter, C., Zwikowics, C., Jamrow, T., Manisseri, C., Somerville, S. C., and Voigt, C. A. 2013. Elevated early callose deposition results in complete penetration resistance to powdery mildew in *Arabidopsis*. Plant Physiol. 161:1433-1444.

Eynck, C., Koopmann, B., Karlovsky, P., and von Tiedemann, A. 2009. Internal resistance in winter oilseed rape inhibits systemic spread of the vascular pathogen *Verticillium longisporum*. Phytopathology 99:802-811.

Fradin, E. F., and Thomma, B. P. H. J. 2006. Physiology and molecular aspects of Verticillium wilt disease caused by *V. dahliae* and *V. albo-atrum*. Mol. Plant Pathol. 7:71-86.

Fu, Z. Q., and Dong, X. 2013. Systemic acquired resistance: Turning local infection into global defense. Annu. Rev. Plant Biol. 64:839-863.

Fu, Z. Q., Yan, S., Saleh, A., Wang, W., Ruble, J., Oka, N., Mohan, R., Spoel, S. H., Tada, Y., Zheng, N., and Dong, X. 2012. NPR3 and NPR4 are receptors for the immune signal salicylic acid in plants. Nature 486:228-232.

Fung, R. W. M., Gonzalo, M., Fekete, C., Kovacs, L. G., He, Y., Marsh, E., McIntyre, L. M., Schachtman, D. P., and Qiu, W. P. 2008. Powdery mildew induces defense-oriented reprogramming of the transcriptome in a susceptible but not in a resistant grapevine. Plant Physiol. 146:236-249.

Gao, W., Long, L., Zhu, L. F., Xu, L., Gao, W. H., Sun, L. Q., Liu, L. L., and Zhang, X. L. 2013. Proteomic and virus-induced gene silencing (VIGS) analyses reveal that gossypol, brassinosteroids and jasmonic acid contribute to the resistance of cotton to *Verticillium dahliae*. Mol. Cell. Proteomics 12:3690-3703.

Gao, X. Q., Wheeler, T., Li, Z. H., Kenerley, C. M., He, P., and Shan, L. B. 2011. Silencing *GhNDR1* and *GhMKK2* compromises cotton resistance to Verticillium wilt. Plant J. 66:293-305.

Glazebrook, J. 2005. Contrasting mechanisms of defense against biotrophic and necrotrophic pathogens. Annu. Rev. Phytopathol. 43:205-227.

Gold, J., and Robb, J. 1995. The role of the coating response in Craigella tomatoes infected with *Verticillium dahliae*, races 1 and 2. Physiol. Mol. Plant Pathol. 47:141-157.

Grant, M., and Lamb, C. 2006. Systemic immunity. Curr. Opin. Plant Biol. 9:414-420.

Hamann, T. 2012. Plant cell wall integrity maintenance as an essential component of biotic stress response mechanisms. Front. Plant Sci. 3:77.

Heinlein, M. 2002. The spread of tobacco mosaic virus infection: Insights into the cellular mechanism of RNA transport. Cell. Mol. Life Sci. 59:58-82.

Heinz, R., Lee, S. W., Saparno, A., Nazar, R. N., and Robb, J. 1998. Cyclical systemic colonization in Verticillium-infected tomato. Physiol. Mol. Plant Pathol. 52:385-396.

Hückelhoven, R. 2007. Cell wall-associated mechanisms of disease resistance and susceptibility. Annu. Rev. Phytopathol. 45:101-127.

Jacobs, A. K., Lipka, V., Burton, R. A., Panstruga, R., Strizhov, N., and Schulze-Lefert, P. 2003. An *Arabidopsis* callose synthase, *GSL5*, is required for wound and papillary callose formation. Plant Cell 15:2503-2513.

Jones, D., Blancaflor, E., Kochian, L., and Gilroy, S. 2006. Spatial coordination of aluminium uptake, production of reactive oxygen

species, callose production and wall rigidification in maize roots. Plant Cell Environ. 29:1309-1318.
Jones, J. D., and Dangl, J. L. 2006. The plant immune system. Nature 444: 323-329.
Keen, N. T. 1992. The molecular biology of disease resistance. Plant Mol. Biol. 19:109-122.
Lamb, C., and Dixon, R. A. 1997. The oxidative burst in plant disease resistance. Annu. Rev. Plant Physiol. 48:251-275.
Lee, J. Y., Wang, X., Cui, W., Sager, R., Modla, S., Czymmek, K., Zybaliov, B., van Wijk, K., Zhang, C., Lu, H., and Lakshmanan, V. 2011. A plasmodesmata localized protein mediates crosstalk between cell-to-cell communication and innate immunity in *Arabidopsis*. Plant Cell 23: 3353-3373.
Li, H., and Durbin, R. 2009. Fast and accurate short read alignment with Burrows-Wheeler Transform. Bioinformatics 25:1754-1760.
Livak, K. J., and Schmittgen, T. D. 2001. Analysis of relative gene expression data using real-time quantitative PCR and the $2^{-\Delta\Delta CT}$ method. Methods 25:402-408.
López-Cruz, J., Crespo-Salvador, Ó., Fernández-Crespo, E., García-Agustín, P., and González-Bosch, C. 2017. Absence of Cu-Zn-superoxide dismutase BCSOD1 reduces *Botrytis cinerea* virulence in Arabidopsis and in tomato plants, which reveals interplay among ROS, callose and signaling pathways. Mol. Plant Pathol. 18:16-31.
Ma, Z. Y., Wang, X. F., Zhang, G. Y., Liu, S. Q., Liu, J. L., and Sun, J. Z. 2000. Genetic studies of Verticillium wilt resistance among different types of Sea Island cottons. Acta Agron. Sin. 26:315-321.
Mai, V. C., Bednarski, W., Borowiak-Sobkowiak, B., Wilkaniec, B., Samardakiewicz, S., and Morkunas, L. 2013. Oxidative stress in pea seedling leaves in response to *Acyrthosiphon pisum* infestation. Phytochemistry 93: 49-62.
Malinovsky, F. G., Fangel, J. U., and Willats, W. G. T. 2014. The role of the cell wall in plant immunity. Front. Plant Sci. 5:178-189.
Mol, L., Schol, K., and Vos, J. 1995. Effects of crop rotation and removal of crop debris on the soil population of two isolates of *Verticillium dahliae*. Plant Pathol. 44:1070-1074.
Moore, J. W., Loake, G. J., and Spoel, S. H. 2011. Transcription dynamics in plant immunity. Plant Cell 23:2809-2820.
Mysore, K. S., Crasta, O. R., Tuori, R. P., Folkerts, O., Swirsky, P. B., and Martin, G. B. 2002. Comprehensive transcript profiling of *Pto*- and *Prf*-mediated host defense responses to infection by *Pseudomonas syringae* pv. *tomato*. Plant J. 32:299-315.
Pasche, J. S., Mallik, I., Anderson, N. R., and Gudmestad, N. C. 2013. Development and validation of a real-time PCR assay for the quantification of *Verticillium dahliae* in potato. Plant Dis. 97:608-618.
Pomar, F., Novo, M., Bernal, M. A., Merino, F., and Barcelo, A. R. 2004. Changes in stem lignins (monomer composition and crosslinking) and peroxidase are related with the maintenance of leaf photosynthetic integrity during Verticillium wilt in *Capsicum annuum*. New Phytol. 163:111-123.
Robb, J., Shittu, H., Soman, K. V., Kurosky, A., and Nazar, R. N. 2012. Arsenal of elevated defense proteins fails to protect tomato against *Verticillium dahliae*. Planta 236:623-633.
Scalschi, L., Sanmartín, M., Camañes, G., Troncho, P., Sánchez-Serrano, J. J., García-Agustín, P., and Vicedo, B. 2015. Silencing of OPR3 in tomato reveals the role of OPDA in callose deposition during the activation of defense responses against *Botrytis cinerea*. Plant J. 81:304-315.
Schenk, P. M., Kazan, K., Manners, J. M., Anderson, J. P., Simpson, R. S., Wilson, I. W., Somerville, S. C., and Maclean, D. J. 2003. Systemic gene expression in Arabidopsis during an incompatible interaction with *Alternaria brassicicola*. Plant Physiol. 132:999-1010.
Schenk, S. T., Hernández-Reyes, C., Samans, B., Stein, E., Neumann, C., Schikora, M., Reichelt, M., Mithöfer, A., Becker, A., Kongel, K. H., and Schikora, A. 2014. *N*-Acyl-Homoserine lactone primes plants for cell wall reinforcement and induces resistance to bacterial pathogens via the salicylic acid/oxylipin pathway. Plant Cell 26:2708-2723.
Schoelz, J. E., Harries, P. A., and Nelson, R. S. 2011. Intracellular transport of plant viruses: Finding the door out of the cell. Mol. Plant 4:813-831.
Schwessinger, B., and Ronald, P. C. 2012. Plant innate immunity: Perception of conserved microbial signatures. Annu. Rev. Plant Biol. 63:451-482.
Sevilem, I., Miyashima, S., and Helariutta, Y. 2013. Cell-to-cell communication via plasmodesmata in vascular plants. Cell Adhes. Migr. 7:27-32.
Shah, J. 2009. Plants under attack: Systemic signals in defense. Curr. Opin. Plant Biol. 12:459-464.
Sink, K. C., and Grey, W. E. 1999. A root-injection method to assess Verticillium wilt resistance of peppermint and its use in identifying resistant somaclones of cv. Black Mitcham. Euphytica 106:223-230.
Su, X., Qi, X., and Cheng, H. 2014. Molecular cloning and characterization of enhanced disease susceptibility 1 (EDS1) from *Gossypium barbadense*. Mol. Biol. Rep. 41:3821-3828.
Sun, Q., Jiang, H., Zhu, X., Wang, W., He, X., Shi, Y., Yuan, Y., Du, X., and Cai, Y. 2013. Analysis of sea-island cotton and upland cotton in response to *Verticillium dahliae* infection by RNA sequencing. BMC Genomics 14:852.
Tao, Y., Xie, Z., Chen, W., Glazebrook, J., Chang, H. S., Han, B., Zhu, T., Zou, G., and Katagirif, F. 2003. Quantitative nature of Arabidopsis responses during compatible and incompatible interactions with the bacterial pathogen *Pseudomonas syringae*. Plant Cell 15:317-330.
Ueki, S., and Citovsky, V. 2011. To gate, or not to gate: Regulatory mechanisms for intercellular protein transport and virus movement in plants. Mol. Plant 4:782-793.
Vallad, G. E., and Subbarao, K. V. 2008. Colonization of resistant and susceptible lettuce cultivars by a green fluorescent protein-tagged isolate of *Verticillium dahliae*. Phytopathology 98:871-885.
Valsesia, G., Gobbin, D., Patocchi, A., Vecchione, A., Pertot, I., and Gessler, C. 2005. Development of a high-throughput method for quantification of *Plasmopara viticola* DNA in grapevine leaves by means of quantitative real-time polymerase chain reaction. Phytopathology 95:672-678.
van Loon, L. C., Rep, M., and Pieterse, C. M. J. 2006. Significance of inducible defense-related proteins in infected plants. Annu. Rev. Phytopathol. 44:135-162.
Vlot, A. C., Dempsey, D. A., and Klessig, D. F. 2009. Salicylic acid, a multifaceted hormone to combat disease. Annu. Rev. Phytopathol. 47: 177-206.
von Röpenack, E., Parr, A., and Schulze-Lefert, P. 1998. Structural analyses and dynamics of soluble and cell wall-bound phenolics in a broad spectrum resistance to the powdery mildew fungus in barley. J. Biol. Chem. 273:9013-9022.
Waigmann, E., Lucas, W. J., Citovsky, V., and Zambryski, P. 1994. Direct functional assay for tobacco mosaic virus cell-to-cell movement protein and identification of a domain involved in increasing plasmodesmal permeability. Proc. Natl. Acad. Sci. U.S.A. 91:1433-1437.
Wang, X., Sager, R., Cui, W., Zhang, C., Lu, H., and Lee, J. Y. 2013. Salicylic acid regulates plasmodesmata closure during innate immune responses in *Arabidopsis*. Plant Cell 25:2315-2329.
Wang, Y. X., Wang, S. F., Ma, Z. Y., Zhang, G. Y., and Zhao, J. F. 2007. A new high-efficient cotton graft technique and application. Sci. Agric Sin 40:264-270.
Wendel, J. F., and Cronn, R. C. 2003. Polyploidy and the evolutionary history of cotton. Adv. Agron. 78:139-186.
Wiermer, M., Feys, B. J., and Parker, J. E. 2005. Plant immunity: The *EDS1* regulatory node. Curr. Opin. Plant Biol. 8:383-389.
Wilhelm, S., Sagen, J. E., and Tietz, H. 1972. Resistance to Verticillium wilt transferred from *Gossypium barbadense* to Upland cotton phenotype. Phytopathology 62:798-799.
Wilhelm, S., Sagen, J. E., and Tietz, H. 1974. *Gossypium hirsutum* subsp. *mexicanum* var nervosum, Leningrad strain–a source of resistance to Verticillium wilt. Phytopathology 64:931-939.
Xu, L., Zhou, L. F., Tu, L. L., Lin, Z. X., Yuan, D. J., Jin, L., and Zhang, X. L. 2011. Lignin metabolism has a central role in the resistance of cotton to the wilt fungus *Verticillium dahliae* as revealed by RNA-Seq-dependent transcriptional analysis and histochemistry. J. Exp. Bot. 62: 5607-5621.
Xu, M., Gui, Y. J., Qin, W. Y., Liu, S. Y., Chen, J. Y., and Dai, X. F. 2013. *Verticillium dahliae* labeled with green fluorescent protein gene. Plant Prot. 39:128-133.
Zhang, J. F., Fang, H., Zhou, H. P., Sanogo, S., and Ma, Z. Y. 2014. Genetics, breeding, and marker-assisted selection for Verticillium wilt resistance in cotton. Crop Sci. 54: 1289-1303.
Zhang, Y., Wang, X. F., Ding, Z. G., Ma, Q., Zhang, G. R., Zhang, S. L., Li, Z. K., Wu, L. Q., Zhang, G. Y., and Ma, Z. Y. 2013. Transcriptome profiling of *Gossypium barbadense* inoculated with *Verticillium dahliae* provides a resource for cotton improvement. BMC Genomics 14:637.
Zhao, P., Zhao, Y. L., Jin, Y., Zhang, T., and Guo, H. S. 2014. Colonization process of *Arabidopsis thaliana* roots by a green fluorescent protein–tagged isolate of *Verticillium dahliae*. Protein Cell 5:94-98.

AUTHOR-RECOMMENDED INTERNET RESOURCE

CottonGen database: http://www.cottongen.org